RESEARCH ARTICLE

WILEY

Intestinal inflammation alters mucosal carbohydrate foraging and monosaccharide incorporation into microbial glycans

Gisela Adrienne Weiss[1,2] | Thomas Grabinger[1] | Jesus Glaus Garzon[1] | Tobias Hasler[1] | Anna Greppi[3] | Christophe Lacroix[3] | Nikolay Khanzhin[4] | Thierry Hennet[1]

[1]Institute of Physiology, University of Zurich, Zurich, Switzerland

[2]Yili Innovation Center Europe, Bronland 12E-1, 6708WH Wageningen, Netherlands

[3]Laboratory of Food Biotechnology, Department of Health Sciences and Technology, ETH-Zurich, Zurich, Switzerland

[4]Glycom A/S, Hørsholm, Denmark

Correspondence
Thierry Hennet, Institute of Physiology, University of Zurich, Winterthurerstrasse 190, CH-8057 Zurich, Switzerland.
Email: thierry.hennet@uzh.ch

Abstract

Endogenous carbohydrates released from the intestinal mucus represent a constant source of nutrients to the intestinal microbiota. Mucus-derived carbohydrates can also be used as building blocks in the biosynthesis of bacterial cell wall components, thereby influencing host mucosal immunity. To assess the uptake of endogenous carbohydrates by gut microbes in healthy mice and during intestinal inflammation, we applied azido-monosaccharides that can be tracked on bacterial cell walls after conjugation with fluorophores. In interleukin-10 deficient mice, changes in the gut microbiota were accompanied by decreased carbohydrate hydrolase activities and increased lumenal concentrations of host glycan-derived monosaccharides. Tracking of the monosaccharide N-azidoacetylglucosamine (GlcNAz) in caecum bacteria revealed a preferential incorporation of this carbohydrate by *Xanthomonadaceae* in healthy mice and by *Bacteroidaceae* in interleukin-10 deficient mice. These GlcNAz-positive *Bacteroidaceae* fractions mainly belonged to the species *B. acidifaciens* and *B. vulgatus*. Growth of *Bacteroides* species in the presence of specific monosaccharides changed their stimulatory activity toward CD11c^{+} dendritic cells. Expression of activation markers and cytokine production was highest after stimulation of dendritic cells with *B. vulgatus*. The variable incorporation of monosaccharides by related *Bacteroides* species underline the necessity to investigate intestinal bacteria down to the species level when addressing microbiota-host interactions.

KEYWORDS

bacteria, Bacteroides, carbohydrate hydrolase, click chemistry, dendritic cell, GlcNAc, Glycan, interleukin-10, mucin, mucus

1 | INTRODUCTION

The gut microbiota is an inherent component of animal physiology that influences the functions of multiple organ systems. The composition of the gut microbiota is itself under the influence of exogenous factors such as dietary intake, ingested drugs, and endogenous factors such as the immune system and the intestinal mucosa (Weiss & Hennet, 2017). The mucus lining of the gastrointestinal tract provides a protective barrier preventing the direct contact of the epithelium with microbes. This mucus, which is mainly constituted of heavily

glycosylated mucin proteins (Davies et al., 2016), also represents a source of carbohydrates used by several intestinal microbes as nutrients.

The secretion of mucins and the resulting thickness of the mucus layer varies along the segments of the gastrointestinal tract. The mucus is thin and patchy in the small intestine, while thick and stratified in the large intestine that harbours most of the microbiota. The mucus plays an ambivalent role in the relationship of the host to its microbiota. Whereas the stratified inner mucus layer acts as a barrier (Johansson et al., 2008), the outer gel-like layer creates a bacterial habitat, which enables the microbial foraging of host glycans (Hansson, 2012). Bacterial lipopolysaccharide (LPS), lipoteichoic acid and cytokines such as tumour necrosis factor (TNF)-α and interleukin (IL)-23 regulate not only mucin expression (Ahn et al., 2005; Hokari et al., 2005), but also the expression of glycosyltransferases, such as the fucosyltransferase FUT2, which increases the fucosylation of intestinal mucins (Goto et al., 2014; Pickard et al., 2014).

Glycans make up to 80% of the mucus mass and are rich in N-acetylgalactosamine (GalNAc), galactose (Gal), N-acetylglucosamine (GlcNAc), sialic acid (Sia), and fucose (Fuc) (Bergstrom & Xia, 2013). Several bacterial taxa express carbohydrate hydrolases (El Kaoutari, Armougom, Gordon, Raoult, & Henrissat, 2013) that liberate monosaccharides from intestinal mucins, thereby providing nutrients to carbohydrate-fermenting microbes. Carbohydrate hydrolases are decisive for the survival of specific bacterial groups, as shown by the decreased fitness of a mutant *Bacteroides thetaiotaomicron* lacking polysaccharide-utilisation loci (Martens, Chiang, & Gordon, 2008).

In addition to their nutritional value, mucin-derived carbohydrates can also be used as building blocks in the biosynthesis of bacterial cell wall components such as peptidoglycan, lipo- and capsular polysaccharides, which contribute to the activation of host immunity. Alternatively, carbohydrates can also be incorporated into cell wall structures to evade immune recognition through molecular mimicry. For example, *Neisseria* spp. and *Haemophilus influenzae* can integrate sialic acid into their lipooligosaccharides to imitate human antigens (Harvey, Swords, & Apicella, 2001) and *Staphylococcus aureus* employs protein modifications with GlcNAc to escape host defences (Thomer et al., 2014).

Despite the established effects of mucosal carbohydrates on the intestinal microbiota (Huang, Chassard, Hausmann, von Itzstein, & Hennet, 2015; Ng et al., 2013), little is known about the identity of bacterial taxa incorporating mucin-derived carbohydrates into their cell wall. To address this question, we applied traceable azido-monosaccharides that can be detected within the bacterial cell wall via conjugation with fluorophores (Dumont, Malleron, Awwad, Dukan, & Vauzeilles, 2012). Using interleukin-10 (*Il10*) deficient mice as model, we studied the fate of monosaccharides in the healthy gut and during intestinal inflammation, which affects the release of carbohydrates from the intestinal mucus. This work underscored the species-dependent incorporation of carbohydrates in the gut microbiota of wildtype (WT) and *Il10*$^{-/-}$ mice.

2 | RESULTS

2.1 | Mucosal glycan utilisation in caecum of WT and *Il10*$^{-/-}$ mice

IL-10 suppresses the biosynthesis of pro-inflammatory cytokines by macrophages, natural killer cells and T cells. Mice lacking *Il10* develop enterocolitis due to the failure to dampen the continuous stimulation of the intestinal immune system by enteric antigens (Kuhn, Lohler, Rennick, Rajewsky, & Muller, 1993). Colonic inflammation in *Il10*$^{-/-}$ mice is accompanied by a loss of microbial diversity and richness paralleled with a relative expansion of Proteobacteria (Lupp et al., 2007; Maharshak et al., 2013). The resulting changes in microbial composition are likely to affect bacterial metabolic and biosynthetic pathways, such as the extraction and utilisation of mucosal carbohydrates by specific bacterial taxa. Already at 8–10 weeks of age, *Il10*$^{-/-}$ mice presented a significant colon inflammation featuring shortening of colon length, leukocyte infiltration, local pro-inflammatory cytokine secretion, cryptitis, loss of goblet cells and epithelial damage (Grabinger et al., 2019). At this stage, we assessed changes in mucosal carbohydrate extraction by measuring the major carbohydrate hydrolase activities in the caecum of healthy WT mice and colitic *Il10*$^{-/-}$ mice using colorimetric assays. Some activities, such as α-galactosidase, α- and β-N-acetylglucosaminidase, α- and β-fucosidase were decreased in *Il10*$^{-/-}$ mice, while β-galactosidase and α-sialidase activities remained unchanged (Figure 1a). Given the decrease in carbohydrate hydrolases found in *Il10*$^{-/-}$ mice, we expected a similar decrease in the lumenal levels of monosaccharides released into the caecum. Surprisingly, we detected increased concentrations of the monosaccharides Gal, GalNAc, GlcNAc, Fuc, and the sialic acids N-acetylneuraminic acid (Neu5Ac), N-glycolylneuraminic acid (Neu5Gc), and N-acetyl-9-O-acetylneuraminic acid (Neu5,9Ac$_2$), but not glucose (Glc) in *Il10*$^{-/-}$ mice (Figure 1b). Whereas Glc is mainly derived from dietary fibres, the other monosaccharides represented common building blocks of mucin O-glycans (Koropatkin, Cameron, & Martens, 2012; Thomsson et al., 2012). The monosaccharide galactosamine (GalN) was also increased in the caecum lumen of *Il10*$^{-/-}$ mice, although this carbohydrate is not a constituent of mucin O-glycans.

The concomitant decreased carbohydrate hydrolase activity and increased monosaccharide concentrations pointed to a shift in carbohydrate foraging in *Il10*$^{-/-}$ mice. The increased availability of monosaccharides from intestinal glycans likely influenced the composition of the gut microbiota by providing additional nutrients to specific bacterial taxa. To identify the bacterial groups mainly affected by the increased monosaccharide concentrations, we focused on GlcNAc, which showed the highest increase among the mucin-derived carbohydrates in the caecum lumen (Figure 1b).

2.2 | Incorporation of exogenous monosaccharides by microbial communities

To assess the impact of GlcNAc on the intestinal microbiota, the natural monosaccharide was used as well as its azido derivative to enable
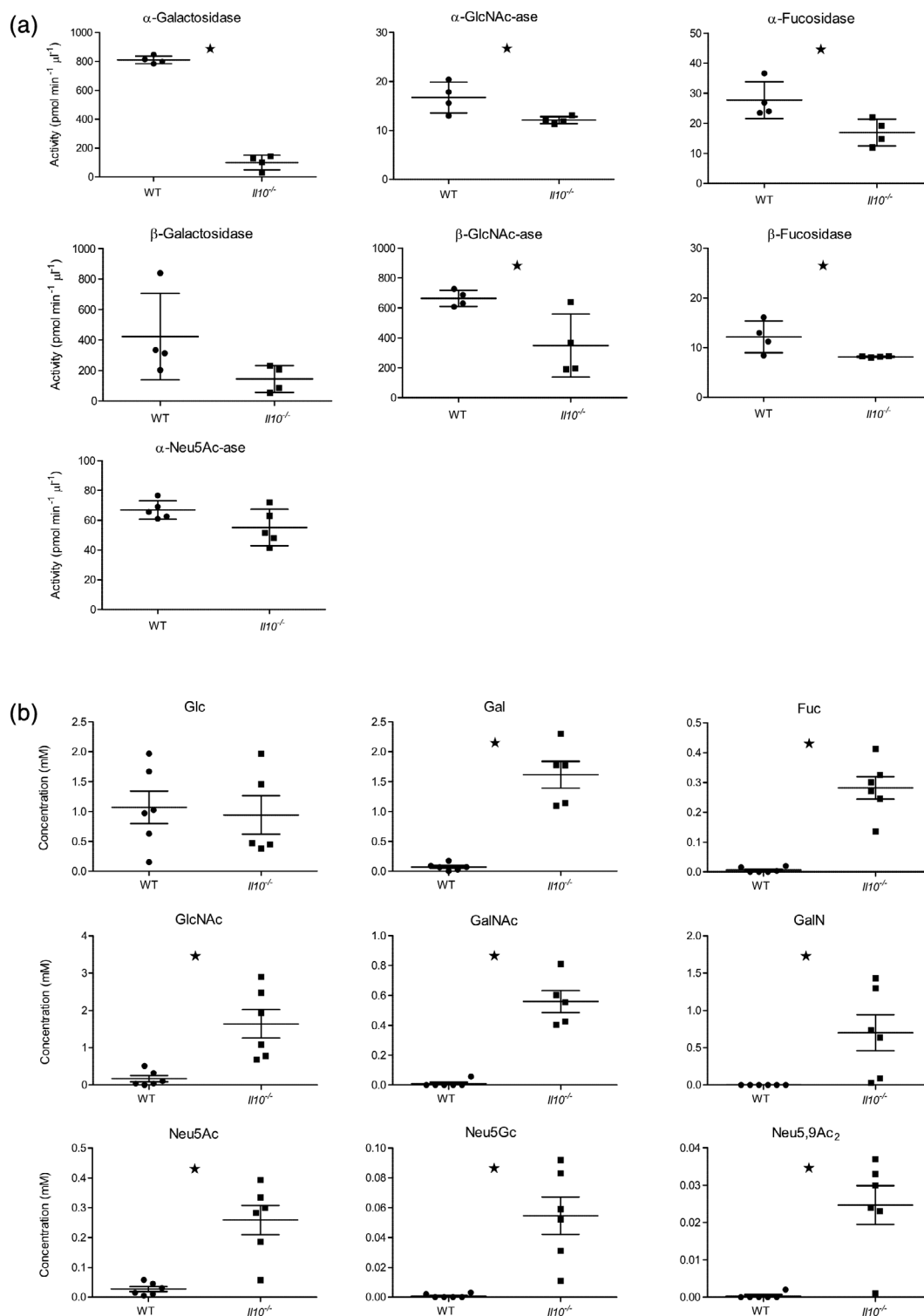
FIGURE 1 Carbohydrates released in caecum fluid of WT and *Il10*$^{-/-}$ mice. (a) Carbohydrate hydrolase activities in 8–10 weeks old mice were measured in caecum fluid by colorimetric assays. Data are shown as mean and standard deviation from 4 to 5 mice per group. (b) Monosaccharide concentrations of core and terminal glycan monosaccharides were determined by HPLC. Glucosamine was not detected in any of the samples. Fuc, fucose; Gal, galactose; GalN, galactosamine; GalNAc, *N*-acetylgalactosamine; Glc, glucose; GlcNAc, *N*-acetylglucosamine; Neu5Ac, 5-*N*-acetylneuraminic acid; Neu5,9Ac2, 5-*N*-acetyl-9-*O*-acetylneuraminic acid; Neu5Gc, 5-*N*-glycolylneuraminic acid. Data represent the mean and standard deviation from 5 to 6 mice investigated at different time points. Statistical significance was determined by unpaired *t*-test (*, $p < .05$)

the subsequent identification of bacteria having incorporated this monosaccharide on their surface. After isolation of the caecum microbiota from mice under oxygen free conditions (Hungate, 1969), we compared the effect of GlcNAc and its azido derivative *N*-azidoacetylglucosamine (GlcNAz) on the microbial composition by supplementing anaerobic bacterial cultures with GlcNAc, GlcNAz or Glc as control. The bacterial composition was analysed by 16S rRNA sequencing before and after 6 hr of culture, which resulted in an increase of OD_{600} by 0.5–0.6. This short incubation time was chosen to minimise the impact of different bacterial growth rates over the incorporation of exogenous monosaccharides. As expected, the composition of the gut microbiota differed between WT and *Il10*$^{-/-}$ mice, with increased relative abundance of *Bacteroidaceae* and *Ruminoccaceae*, and decreased relative abundance of *Helicobacteraceae* in *Il10*$^{-/-}$ mice (Figure 2). Compared with Glc, supplementation of the caecum microbiota with GlcNAc and GlcNAz did not change the microbiota composition significantly in both genotypes when assessed at the family level (Figure 2).

The application of GlcNAz enabled its subsequent labelling after ligation with alkyne-containing fluorophore using click chemistry (Agard, Baskin, Prescher, Lo, & Bertozzi, 2006). Incubation of caecum microbiota with GlcNAz resulted in the incorporation of this monosaccharide on the surface of a portion of the bacterial community as detected by flow cytometry after ligation of the fluorophore

AlexaFluor488-alkyne to the azido group of GlcNAz (Figure 3). Because GlcNAc, and concomitantly GlcNAz, can be converted to other monosaccharides after uptake by bacteria, we also investigated the incorporation of *N*-azidoacetylmannosamine (ManNAz) and N-azidoacetylsialic acid (SiaNAz), which are two possible products of GlcNAz interconversion. These two monosaccharides were also incorporated into caecum bacteria from WT and *Il10*$^{-/-}$ mice as evidenced by increased AlexaFluor488 labelling and flow cytometry (Figure 3). The incorporation of ManNAz was strongest in WT caecum bacteria, whereas SiaNAz was nearly equally incorporated in bacteria from both genotypes.

To identify the caecum bacteria that incorporated GlcNAz, we sorted AlexaFluor488-labelled bacteria from WT and *Il10*$^{-/-}$ derived caecum samples incubated with GlcNAz for 6 hr. The fraction of AlexaFluor488-positive bacteria increased by 6.5-fold and by 8.9-fold in WT and *Il10*$^{-/-}$ samples after incubation with GlcNAz over GlcNAc, respectively. The composition of these AlexaFluor488-positive bacteria was determined by 16S rRNA sequencing. In bacteria derived from WT mice, the families of *Xanthomonadaceae* and *Pseudomonadaceae* were significantly enriched among GlcNAz-positive bacteria. By contrast, in *Il10*$^{-/-}$ mice, the family of *Bacteroidaceae* was the most abundant in GlcNAz-positive samples, reaching up to 64% of all bacteria (Figure 4a). Strikingly, the distribution of *Bacteroidaceae* differed in the two genetical backgrounds. In samples from *Il10*$^{-/-}$ mice, GlcNAz-positive and GlcNAz-negative bacteria did not differ in the number of
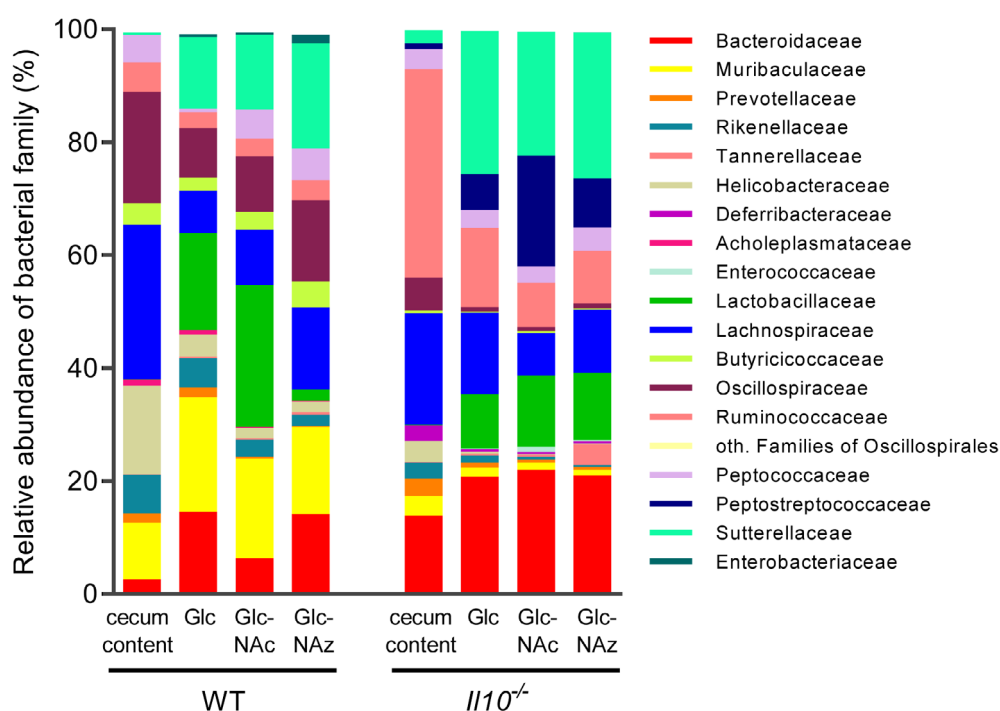
FIGURE 2 GlcNAc and GlcNAz supplementation of the intestinal microbiota induces similar changes as supplementation with Glc. Cultures of caecum slurries from WT and *Il10*$^{-/-}$ mice were supplemented with 1 mM GlcNAc, 1 mM GlcNAz or 1 mM Glc for 6 hr. Microbial changes were analysed by next generation sequencing of 16S rRNA. Graph depicts sequencing analysis at the family level of caecum content and supplemented cultures. Only bacterial taxa representing >1% of total identified sequences are presented. Data show the average percentage of total identified sequences obtained from three mice per group investigated at distinct time points. *Bacteroidaceae*, *Ruminococcaceae*, and *Helicobacteraceae* were significantly different between WT and *Il10*$^{-/-}$ mice in the starting caecum contents as determined by analysis of variance with Bonferroni post hoc test, *p* < .001
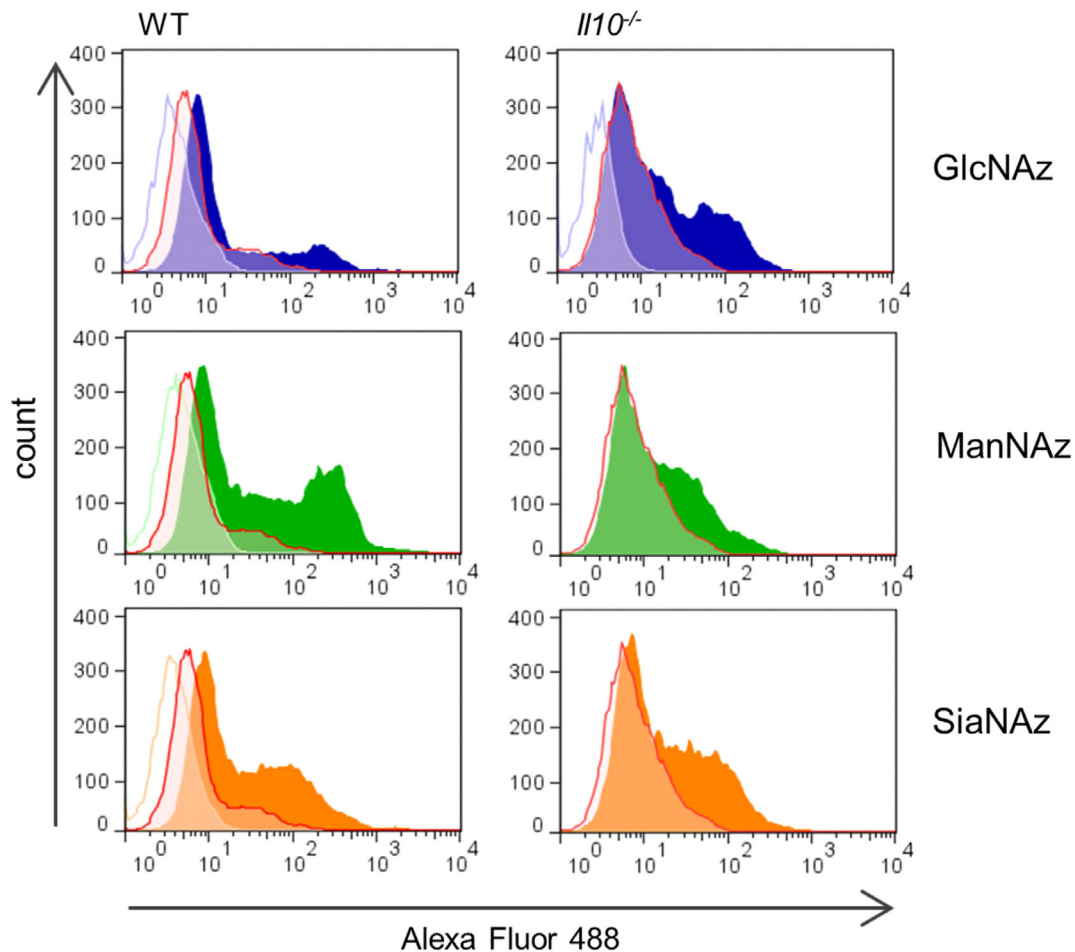
FIGURE 3 Surface presentation of azido sugars of caecum microbiota. Caecum slurries of WT and *Il10*$^{-/-}$ mice were cultured anaerobically and supplemented with GlcNAc, GlcNAz, ManNAz or SiaNAz for 6 hr, then stained with A488-labelled alkyne dye prior to analysis by flow cytometry. Azido sugar-supplemented bacteria not labelled with alkyne dye were used as a second negative control. GlcNAc-supplemented bacteria (red lines), GlcNAz-supplemented bacteria (alkyne-A488 labelled, dark blue; unlabelled, light blue lines), ManNAz-supplemented bacteria (alkyne-A488 labelled, dark green; unlabelled, light green lines), SiaNAz-supplemented bacteria (alkyne-A488 labelled, dark orange; unlabelled, light orange lines). The data shown are representative of three independent experiments

bacterial families, but in the abundance of each family. Principal coordinates analysis confirmed that the differences between the two sorted bacterial groups did not occur in respect to the number of identified OTUs, but due to the unequal abundances of the OTUs in the two groups. This can be seen through the clustering of weighted Unifrac distances along principal coordinate 1 in the *Il10*$^{-/-}$ background. In WT mice, weighted Unifrac distances did not yie

d GlcNAz-specific clusters (Figure S1). Closer examination of the bacteria identified in the GlcNAz-positive fractions revealed that all members of the *Bacteroidaceae* family belonged to the genus *Bacteroides* with *B. acidifaciens* and *B. vulgatus* being the dominant species (Figure 4b). The distribution of these two *Bacteroides* species in WT and *Il10*$^{-/-}$ mouse samples was validated by real-time quantitative PCR using primers specific for the *recA* gene of *B. acidifaciens* and the sialidase gene *bv-f266* of *B. vulgatus*. The constant levels of *B. vulgatus* in WT samples and the increased abundance of *B. vulgatus* and *B. acidifaciens* in *Il10*$^{-/-}$ samples enriched for GlcNAz incorporation was confirmed by the PCR analysis (Figure S2).

2.3 | Incorporation of monosaccharides by *Bacteroides* species

Several *Bacteroides* are efficient carbohydrate foragers (Martens et al., 2011), although the expression of carbohydrate hydrolases and carbohydrate transporters varies between *Bacteroides* species (Ng et al., 2013). We therefore compared the uptake and incorporation of GlcNAz with pure cultures of *B. acidifaciens* and *B. vulgatus*. We included two additional *Bacteroides* species, *B. thetaiotaomicron* and *B. intestinalis*, and we also compared the incorporation of GlcNAz with that of ManNAz and SiaNAz in the four bacterial species. These azido-monosaccharides were added to growth medium containing Glc as a main carbohydrate source. The incorporation of the monosaccharide derivatives was quantified by flow cytometry after reaction of AlexaFluor488-alkyne with azido groups by click chemistry. GlcNAz was efficiently incorporated into surface glycans of the four *Bacteroides* species investigated (Figure 5). This finding supports the notion that these *Bacteroides* species compete for GlcNAz as a carbon source

(a)

(b)
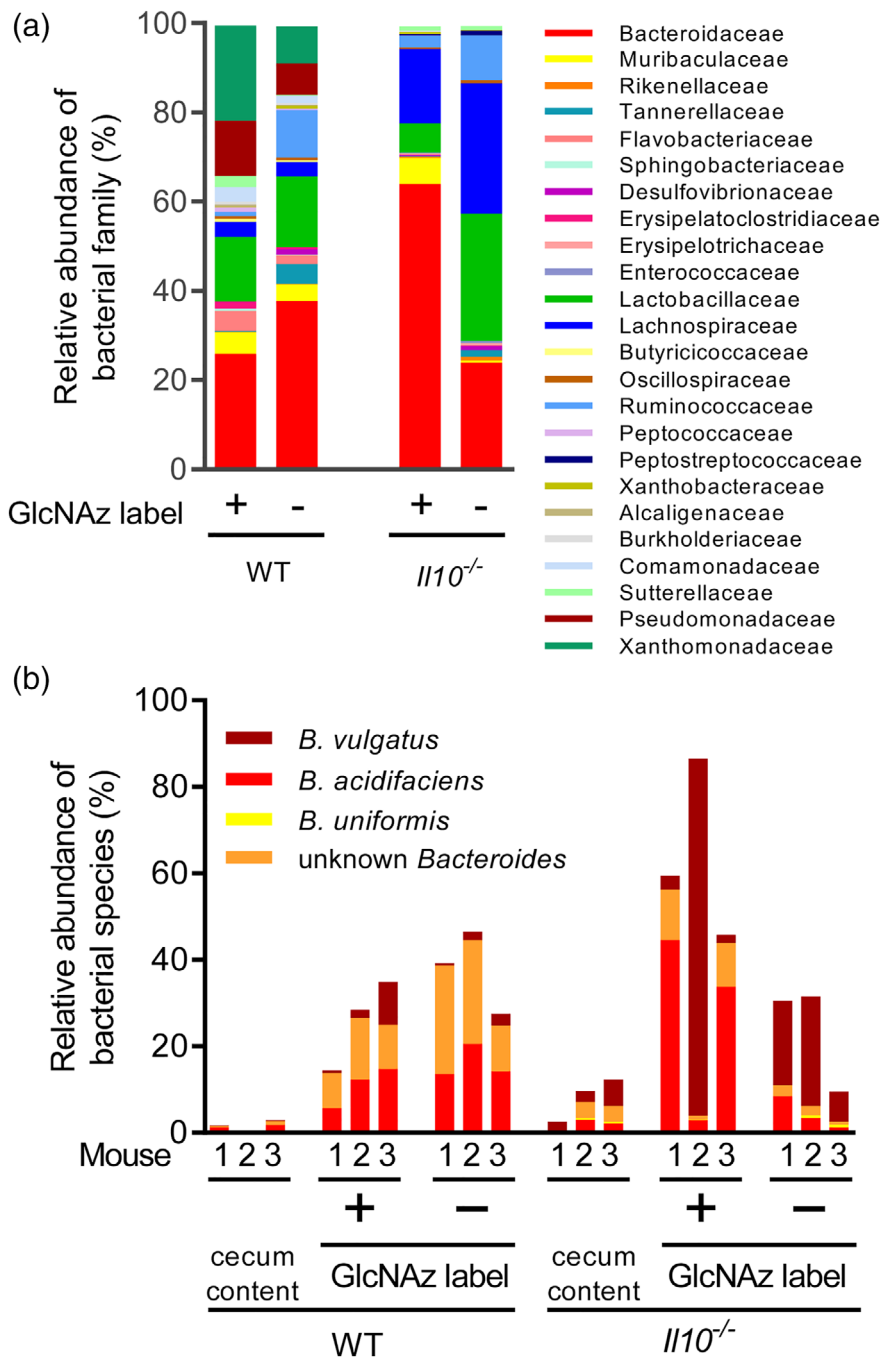
FIGURE 4 Composition of azide-label-positive and azide-label-negative bacteria. (a) 16S rRNA sequencing analysis of GlcNAz-supplemented caecum bacteria sorted as azide-label-positive and azide-label-negative. Sequencing data from WT and $Il10^{-/-}$ mice are shown at family level. Only bacterial taxa representing >1% of total identified sequences are presented. Data show the average percentage of total identified sequences obtained from three mice per group investigated at different time points. *Pseudomonadaceae* and *Xanthomonadaceae* were significantly different between GlcNAz-negative and GlcNAz-positive in WT mice and *Bacteroidaceae* were significantly different between GlcNAz-negative and GlcNAz-positive in $Il10^{-/-}$ mice as determined by analysis of variance with Bonferroni post hoc test, $p < .001$. (b). Relative abundance of individual *Bacteroides* species among *Bacteroidaceae* identified by 16S rRNA sequencing analysis in WT- and $Il10^{-/-}$-derived GlcNAz-supplemented and sorted (GlcNAz label +/−) caecum bacteria from WT and $Il10^{-/-}$ mice investigated independently (3 mice per genotype). The relative abundance of the *Bacteroides* species in the original caecum contents expressed against total bacteria is indicated as "caecum content"

and building block for surface glycans. The incorporation of ManNAz was more restricted, given that *B. acidifaciens* hardly presented any ManNAz on its surface while *B. thetaiotaomicron* and *B. vulgatus* efficiently presented this monosaccharide derivative on their surface. The incorporation of SiaNAz in surface glycans was even more selective, as only *B. vulgatus* presented this monosaccharide significantly among the four *Bacteroides* tested (Figure 5). Growth of *B. vulgatus* and *B. acidifaciens* in the absence of Glc in M9 minimal medium demonstrated that both *Bacteroides* species could grow on GlcNAc, whereas *B. vulgatus* could also utilise SiaNAc as carbon sources. By contrast, *B. acidifaciens* could only grow in minimal medium including Glc or GlcNAc. Both species did not proliferate when ManNAc was available as single carbohydrate source (Figure 6). Incorporation of GlcNAz,

ManNAz, and SiaNAz was also investigated in other commensal bacteria including *Escherichia coli, Lactobacillus brevis, Lactobacillus plantarum, Akkermansia muciniphila* and *Barnesiella intestinihominis*. These bacteria however did not expose any of the three monosaccharide derivatives tested on their surface (**data not shown**).

2.4 | Differential activation of dendritic cells by *Bacteroides* species

The selective proliferation of individual *Bacteroides* species in response to monosaccharide availability is likely to influence host immunity, thus possibly affecting the severity of intestinal
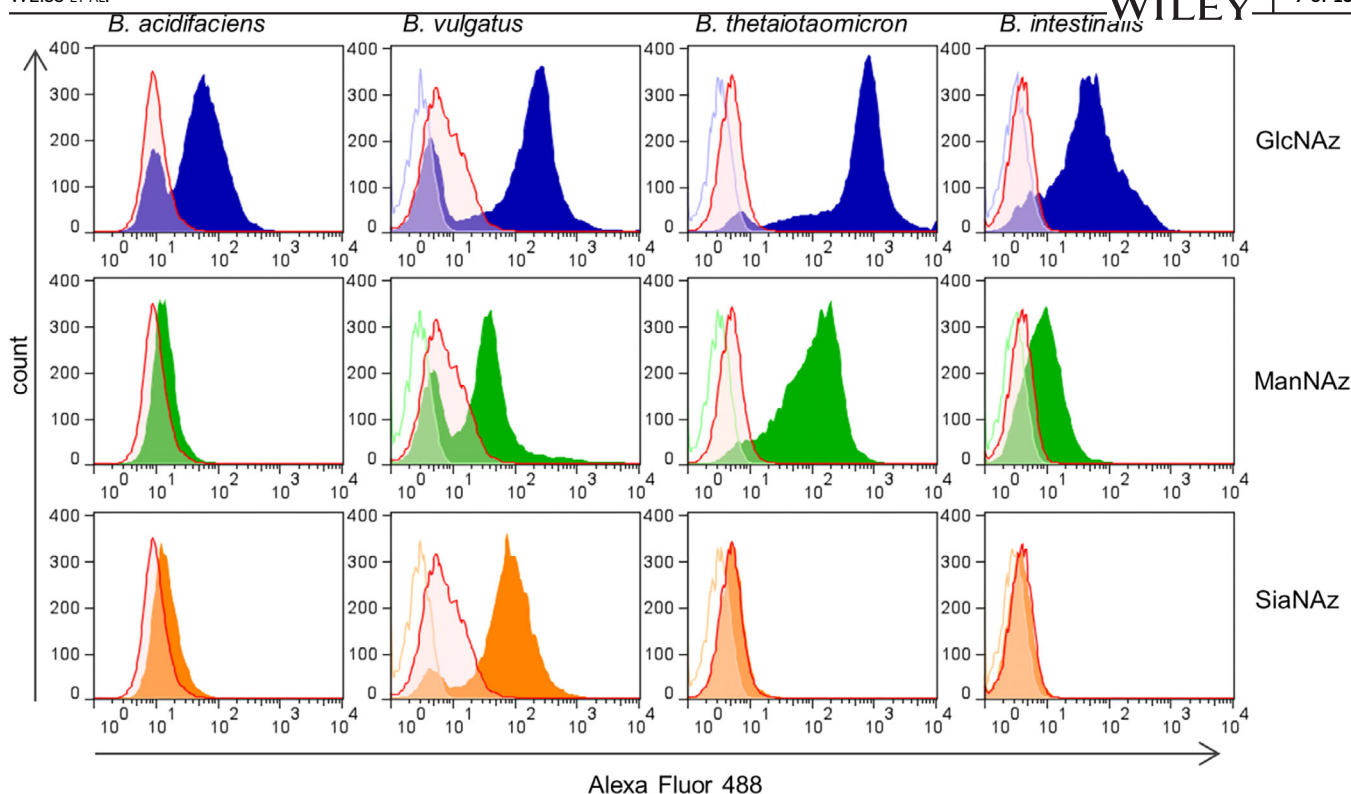
FIGURE 5 Surface presentation of azido sugars by isolated *Bacteroides* species. Isolated *B. acidifaciens*, *B. vulgatus*, *B. thetaiotaomicron* and *B. intestinalis* were cultured and supplemented with GlcNAc, GlcNAz (upper panel), ManNAz (middle panel) or SiaNAz (lower panel) for 6 hr. After fluorophore labelling with alkyne dye, bacteria were analysed by flow cytometry. GlcNAc-supplemented bacteria (red lines), GlcNAz-supplemented bacteria (alkyne-A488 labelled, dark blue; unlabelled, light blue lines), ManNAz-supplemented bacteria (alkyne-A488 labelled, dark green; unlabelled, light green lines), SiaNAz-supplemented bacteria (alkyne-A488 labelled, dark orange; unlabelled, light orange lines). The data shown are representative of three independent experiments
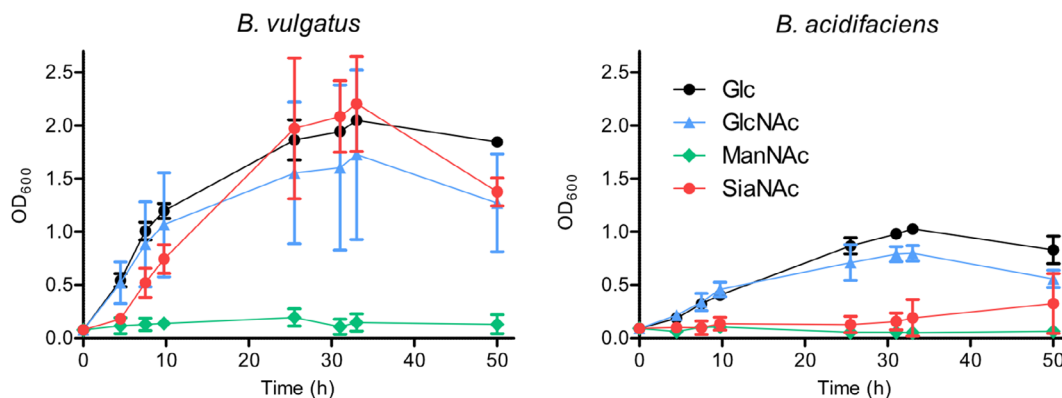
FIGURE 6 Growth of *B. vulgatus* and *B. acidifaciens* in presence of specific monosaccharides. *B. vulgatus* and *B. acidifaciens* at an initial OD_{600} of 0.05 were cultured in Hungate tubes in Glc-free M9 minimal medium supplemented with 20 mM Glc, GlcNAc, ManNAc or SiaNAc. Growth was monitored at OD_{600} until stationary phase was reached. Data represent mean values and standard deviation from three independent experiments

inflammation in *Il10*^{−/−} mice. To assess the effects of monosaccharide incorporation by *Bacteroides* on immune cell functions, we stimulated bone marrow-derived CD11c^{+} dendritic cells with fixed *B. vulgatus* and *B. acidifaciens* grown in medium supplemented with GlcNAc, ManNAc and SiaNAc. With increasing GlcNAc and SiaNAc concentrations, *B. vulgatus* showed a decreased ability to induce the expression

of the activation markers CD40 and CD86 in dendritic cells when compared to bacteria grown in glucose (Figure 7a). By contrast, *B. acidifaciens* hardly induced CD40 and CD86 expression when presented to dendritic cells. Growth in GlcNAc- and SiaNAc containing medium only slightly increased the stimulatory properties of *B. acidifaciens* in respect to CD40 and CD86 expression, respectively
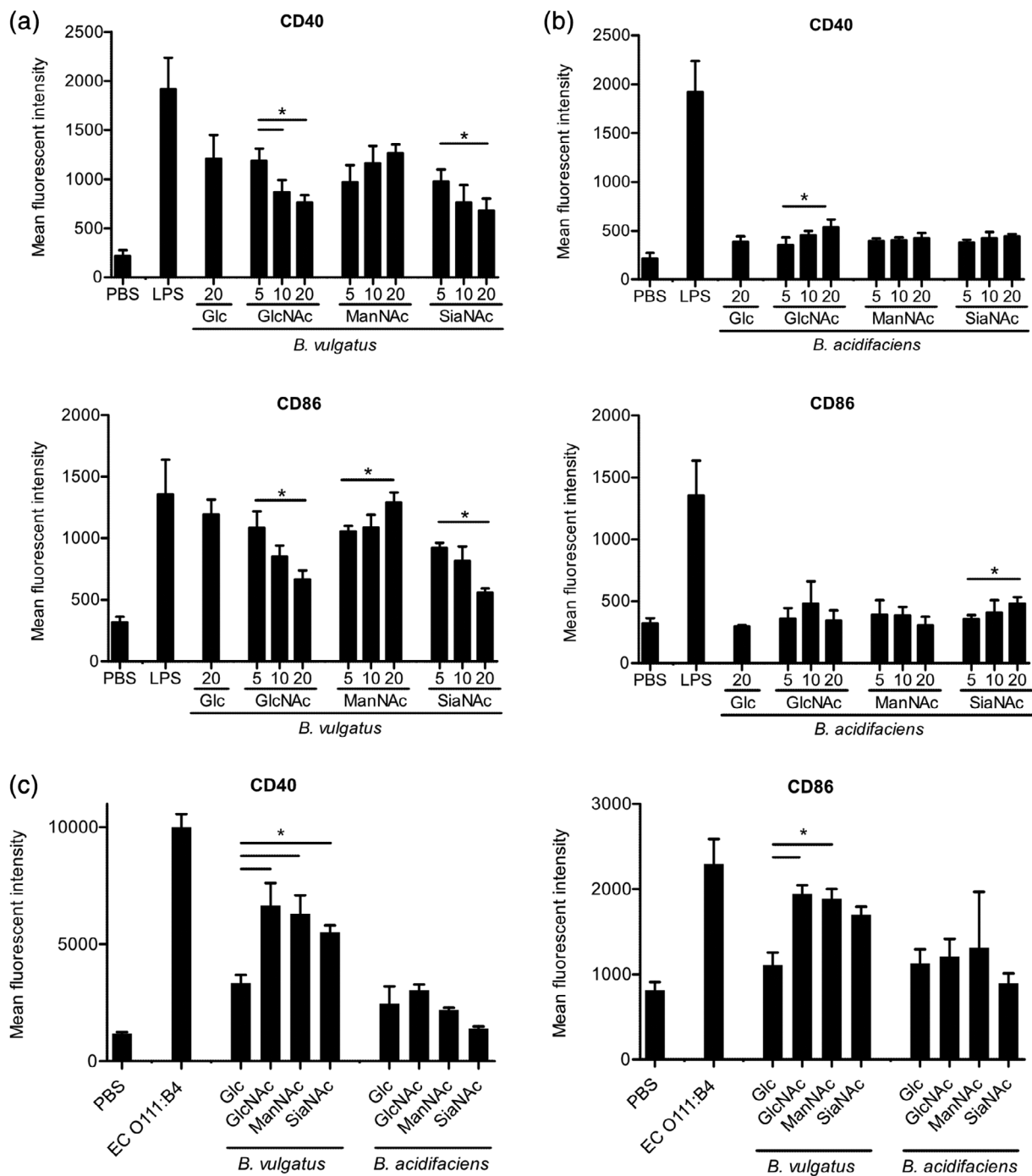
FIGURE 7 Differential activation of bone marrow-derived dendritic cells by *Bacteroides* cultured in presence of monosaccharides. *B. vulgatus* (a) and *B. acidifaciens* (b) were grown 16 hr in the presence of 20 mM Glc or increasing concentrations of GlcNAc, ManNAc or SiaNAc (5, 10 and 20 mM). Dendritic cells were stimulated for 24 hr with PFA-fixed bacteria (ratio of 10 bacteria to 1 cell). PBS and *E. coli* O111:B4 LPS were used as negative and positive controls. (c), Dendritic cells were stimulated for 16 hr with 4 μg/ml of purified LPS from *B. vulgatus* and *B. acidifaciens* cultured in PYG alone or supplemented with 20 mM GlcNAc, ManNAc or SiaNAc. The activation markers CD40 and CD86 were detected by flow cytometry and expressed as mean fluorescent intensity. Data are presented as mean values and standard deviation from three independent experiments. Statistical significance was determined by one-way analysis of variance with a Bonferroni post-hoc test ($p < .05$)

(Figure 7b). The direct stimulation of CD11c$^+$ dendritic cells with purified LPS from *B. vulgatus* and *B. acidifaciens* (Figure S3) cultured in presence of monosaccharides at 20 mM confirmed the differential impact of GlcNAc, ManNAc and SiaNAc supplementation on the stimulatory potential of *B. vulgatus* LPS. As shown for the activation of dendritic cells by whole bacteria, the stimulatory activity of LPS from *B. acidifaciens* was less affected by GlcNAc, ManNAc and SiaNAc supplementation (Figure 7c).

The stimulation ofCD11c$^+$ dendritic cells with *B. vulgatus* grown at elevated GlcNAc- and SiaNAc concentrations also decreased the production of the pro-inflammatory cytokines TNFα and IL-1β when compared to dendritic cells stimulated with *B. vulgatus* grown in glucose-containing medium (Figure 8a). Surprisingly, IL-1β secretion was increased by stimulation with *B. vulgatus* grown at high ManNAc concentration (20 mM) compared to *B. vulgatus* grown in 5 mM ManNAc. Growth at 20 mM GlcNAc or ManNAc also lowered the production of IL-10 in dendritic cells. Elevated monosaccharide concentrations had the opposite effect on IL-17A production stimulated by *B. vulgatus*, an effect that was clearest for GlcNAc and SiaNAc (Figure 8a). As observed for the expression of the activation markers CD40 and CD86, *B. acidifaciens* only induced low levels of TNFα, IL-1β and IL-10 production compared to *B. vulgatus* (Figure 8b). Interestingly, *B. acidifaciens* induced the secretion of IL-17A at similar levels as *B. vulgatus*, although the prior growth of *B. acidifaciens* at varying monosaccharide concentrations did not affect the stimulation of IL-17A production significantly (Figure 8b). These findings
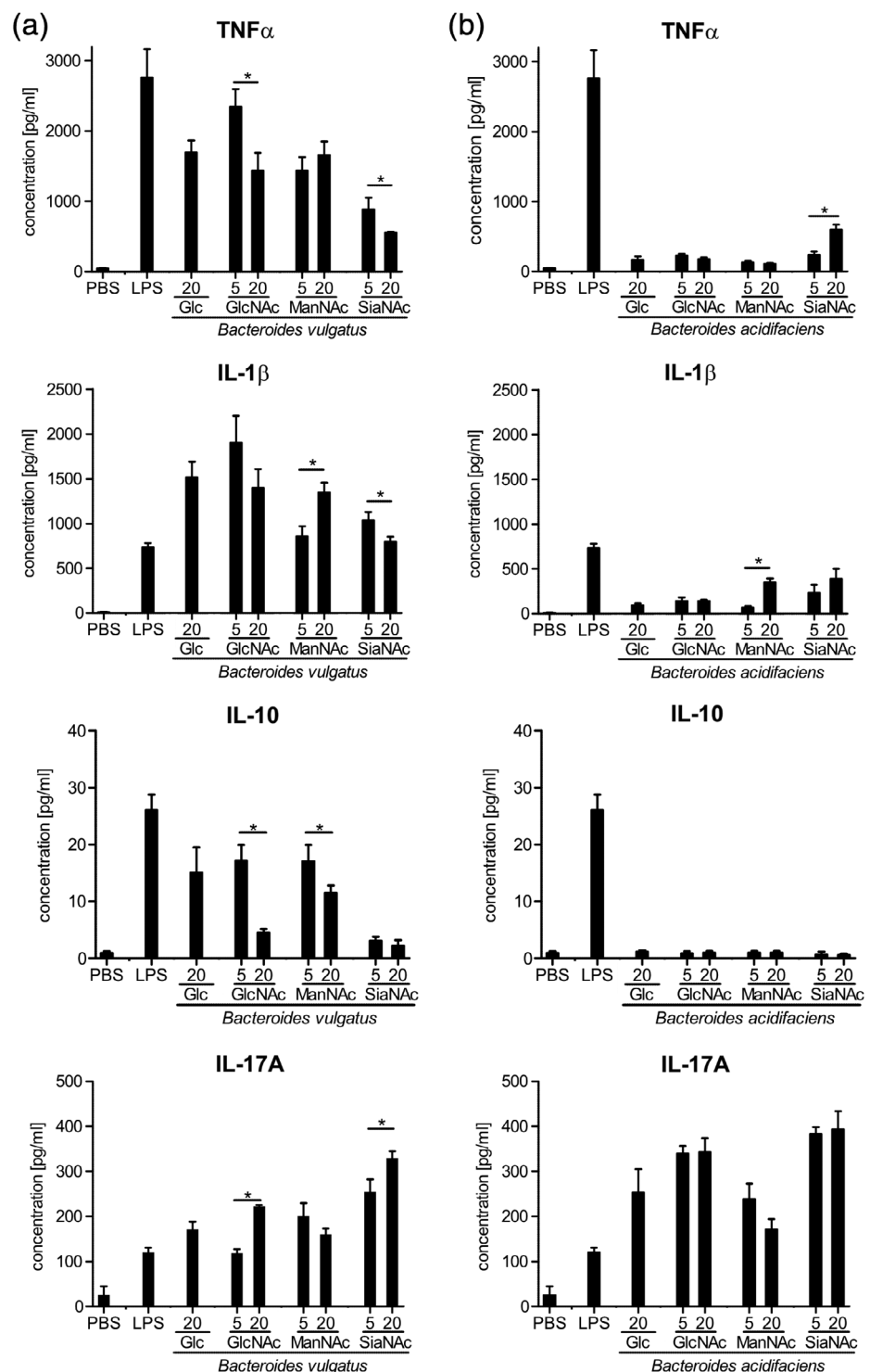
FIGURE 8 Availability of specific carbohydrate substrates in *Bacteroides* cultures leads to a differential cytokine expression profile in bone marrow-derived dendritic cells. Cultures of *B. vulgatus* (a) or *B. acidifaciens* (b) were grown 16 hr in the presence of GlcNAc, ManNAc or SiaNAc in various concentrations (5 and 20 mM) or Glc (20 mM). Harvested bacteria were washed, PFA-fixed and used for a stimulation of dendritic cells for 24 hr with a bacteria-to-cell ratio of 10:1. Unstimulated (PBS) and *E. coli* O111:B4 LPS-stimulated dendritic cells served as controls. Expression of the cytokines TNFα, IL-1β, IL-10 and IL-17A was determined in supernatants by a multiplex immunoassay. Cytokine concentration in pg/ml is presented as mean values and standard deviation (*n* = 3) from independent experiments. Statistical significance (*p* < .05) as indicated by an asterisk was determined by one-way analysis of variance with a Bonferroni post-hoc test

therefore underlined the impact of mucosal monosaccharide availability on the selective expansion of bacterial taxa and on the properties of their surface glycans to differentially stimulate immune cells.

3 | DISCUSSION

This study showed that the intestinal inflammation occurring in $Il10^{-/-}$ mice is accompanied by changes in carbohydrate hydrolase activities and levels of free monosaccharides in the caecum. Lumenal monosaccharides represent nutrients for bacteria able to use these molecules as carbon source. Through the supplementation of caecum bacteria with azido-monosaccharides, we identified selected Bacteroides species as the main bacterial group in $Il10^{-/-}$ mice responding to increased GlcNAc availability by incorporation of the monosaccharide on their surface glycans. The variable responses of specific Bacteroides species to monosaccharide supply and the different effects of Bacteroides species in respect to the activation of dendritic cells underlined the importance to consider bacteria down to the species level when addressing the impact of the microbiota on disease development and progression.

The elevated levels of free monosaccharides detected in $Il10^{-/-}$ mice contrasted with the decreased activity in carbohydrate hydrolases. Considering this lower hydrolase activity, the increased monosaccharide concentrations in the caecum probably reflected a decreased overall consumption of carbohydrates in the inflamed gut of $Il10^{-/-}$ mice. The presence of GalN likely reflected a concomitant increased GalNAc-specific deacetylase activity of bacterial origin in the caecum of $Il10^{-/-}$ mice. The increased occurrence of GalN could also result from the enhanced degradation of intestinal glycosaminoglycans during colitis, which has been shown to be a carbohydrate metabolite entailing direct cytotoxic effects on intestinal cells (Lee, Han, Ryu, & Kim, 2009). Beyond bacterial carbohydrate hydrolases released in the intestinal lumen, host enzymes may also contribute to the increased glycosidic activity, as recently shown by the induction of NEU3 neuraminidase during intestinal inflammation through TLR4-dependent mechanisms (Yang et al., 2017). Changes in carbohydrate cleavage from the intestinal mucosa likely also alter the adhesion of microbes to the mucus by removing ligands or unmasking new binding structures, thereby enabling changes in the microbiota composition. For example, alteration of mucosal glycans may affect the localisation of lactobacilli that express mucus-binding proteins (Etzold & Juge, 2014). Also, the adhesion of pathogenic bacteria such as Campylobacter jejuni and E. coli K99 relies on adhesins binding to fucosylated structures (Mahdavi et al., 2014) and fimbriae binding to sialylated epitopes (Kyogashima, Ginsburg, & Krivan, 1989), respectively. Increased degradation of mucus glycans may also alter intestinal barrier function, although mucus production in the caecum of $Il10^{-/-}$ mice appeared normal by 15 weeks of age.

Our analysis of GlcNAz uptake in caecum bacteria revealed Xanthomonadaceae and Pseudomonadaceae in WT mice, and Bacteroidaceae in $Il10^{-/-}$ mice as the main bacterial families incorporating this monosaccharide on their surface glycans.

Xanthomonadaceae are gram-negative bacteria that express proteins involved in the degradation of N-glycans (Assis et al., 2017). Pseudomonadaceae, like Xanthomonadaceae, belong to the phylum of Proteobacteria. Several members of Pseudomonadaceae express carbohydrate hydrolases, such as PslG in Pseudomonas aeruginosa, which is important for polysaccharide biofilm formation (Baker et al., 2015). In $Il10^{-/-}$ mice, Bacteroidaceae represented the main family in GlcNAz-incorporating bacteria. Metabolic oligosaccharide engineering and fluorophore labelling have successfully been employed before to demonstrate an incorporation of GalNAz in several commensal species including B. fragilis, B. vulgatus, B. thetaiotaomicron and B. ovatus (Geva-Zatorsky et al., 2015). Bacteroidaceae comprise many mucolytic species, such as B. vulgatus and B. thetaiotaomicron (Tailford, Crost, Kavanaugh, & Juge, 2015). A broader combination of catabolic pathways and carbohydrate hydrolases enables nearly all Bacteroides species detected in the human intestine to utilise at least a third of known mucosal glycan structures (Ravcheev & Thiele, 2017). The incorporation of GlcNAz on Bacteroides species is expected considering the inclusion of GlcNAc in the core of lipid A (Raetz & Whitfield, 2002). ManNAc and SiaNAc are by contrast only found in the O-antigen region of LPS or on glycoproteins. Some Bacteroides species express enzymes processing N-acetylneuraminic acid through ManNAc epimerisation (Brigham et al., 2009), which may account for the incorporation of these monosaccharides on surface glycoconjugates. Little is known about the O-antigen structure of the Bacteroides species investigated. The LPS of B. vulgatus consists of multiple O-antigen repeats (Hashimoto et al., 2002), whereas B. thetaiotaomicron appears to only present a short O-antigen on its LPS (Jacobson, Choudhury, & Fischbach, 2018).

In addition to peptidoglycan, LPS and glycoproteins, several Bacteroides species express capsular polysaccharides (Fletcher, Coyne, Villa, Chatzidaki-Livanis, & Comstock, 2009). Some of these capsular polysaccharides exert immune-regulatory effects, such as mitigating intestinal inflammation (Mazmanian, Round, & Kasper, 2008) and inducing T regulatory cells (Neff et al., 2016). The incorporation of azido-monosaccharides in surface glycans, such as capsular polysaccharides, enables the labelling of these glycans and their tracking in the context of antigen presentation and immune cell activation. The different patterns of cytokine expression induced by B. acidifaciens and B. vulgatus in dendritic cells underlined the distinct immune-regulatory properties of these related bacterial species. This variation in cell activation and cytokine response probably reflects the binding of bacterial glycans to different C-type lectins on dendritic cells. The analysis of dendritic cell activation and cytokine production induced by B. acidifaciens and B. vulgatus also emphasises the significant differences in the pro-inflammatory effect of these two species.

Whereas azido-monosaccharides enable the identification of specific bacteria incorporating specific carbohydrates within broad communities, the success of the approach is limited to bacteria that do not cleave the azido group, such as for example by deacetylation. After entering the cell, exogenous GlcNAc is immediately phosphorylated to GlcNAc-6-PO$_4$, enabling the bacterium to distinguish endogenous and exogenous GlcNAc in order to keep the balance between

synthesis and catabolism (Konopka, 2012). GlcNAc-6-PO_4 is often deacetylated before entering glycosylation pathways, although the detection of intact GlcNAz on surface glycans points to alternative pathway for GlcNAz/GlcNAc processing in some bacteria, as previously proposed for *E. coli* (Uehara & Park, 2004). Another drawback of the approach relates to the short period of labelling with azido-monosaccharides. The resulting transitory picture of GlcNAz uptake by intestinal bacteria may not reflect the natural incorporation of mucosal carbohydrate by the gut microbiota at steady-state. Slowly growing bacteria and taxa of low abundance are likely to be missed out, thus restricting the general significance of the results obtained. Despite this limitation, this study showed that bacteria that incorporate specific monosaccharides can be tracked within complex bacterial communities. The variable incorporation of monosaccharides by related *Bacteroides* species, and the variability in cytokine production induced by *B. acidifaciens* and *B. vulgatus* cultured in the presence of different monosaccharides underline the necessity to investigate intestinal bacteria down to the species level when addressing microbiota-host interactions.

4 | EXPERIMENTAL PROCEDURES

4.1 | Mouse models

Mice were of C57BL/6 background. WT and $Il10^{-/-}$ (Kuhn et al., 1993) were bred in house for at least six generations and maintained in a climate-controlled and light-cycled facility. Animals received regular laboratory chow diet (KLIBA extrudat no. 3436, Provimi Kliba, SA, Switzerland) and sterile water *ad libitum*. Mice were investigated at 8–10 weeks of age. All experiments were approved by the Veterinary Office of the Canton of Zurich, Switzerland and carried out in compliance with the Swiss Animal Protection Ordinance.

4.2 | Bacterial species and culture

Bacteroides vulgatus (DSM 1447^T), *Bacteroides intestinalis* (DSM 17393^T), *Bacteroides thetaiotaomicron* (DSM 2079^T), *Bacteroides acidifaciens* (DSM 15896 ^{T}), *Lactobacillus plantarum* subsp. *plantarum* (DSM 20174^T), *Lactobacillus brevis* (DSM 20054^T), *Barnesiella intestinihominis* (DSM 21032^T) and *A. muciniphila* (DSM 22959^T) were obtained from the German Collection of Microorganisms and Cell Cultures (DSMZ, Braunschweig, Germany). Isolation and confirmation of *E. coli* strain EHV2 was described previously (Huang et al., 2015). *Lactobacillus plantarum* subsp. *plantarum* and *L. brevis* were cultured aerobically at 30°C, initially in MRS (De Man, Rogosa and Sharpe) medium (DSMZ, medium no. 11), then transferred to YCFA (yeast extract-casein hydrolysate-fatty acids) medium (Duncan, Hold, Harmsen, Stewart, & Flint, 2002) for supplementation studies. *Escherichia coli* strain EHV2 was cultured and supplemented aerobically at 37°C in M9 minimal medium (Sambrook & Russel, 2001) for supplementation studies and in LB medium for cell stimulation experiments. All other bacteria were manipulated under CO_2 flushing applying Hungate techniques (Hungate, 1969) and cultivated anaerobically in rubber-sealed Hungate tubes at 37°C. *Bacteroides* and *Barnesiella* species were grown and supplemented in PYG (DSMZ, medium no. 104 without glucose) or chopped meat medium (DSMZ, medium no. 78 including haemin and vitamin K_1). *Akkermansia muciniphila* was cultured in modified YCFA medium in which vitamins and fatty acids were omitted, but mucin type II was added (8 mg/100 ml). Bacteria were supplemented with 1 mM GlcNAc, GlcNAz, ManNAz or SiaNAz. Cell density was measured by a spectrophotometer at 600 nm (WPA S1200+, Biochrom).

4.3 | Monosaccharide supplementation of murine microbiota

Euthanized mice were transferred to an anaerobic box (Bugbox M, Baker Ruskinn) and dissected under 5% CO_2 and 0% O_2. The caecum was removed aseptically and its content (portions of about 100 μl) was transferred under CO_2 flushing to PYG medium (0.25% m/v, caecum content in corresponding liquid growth medium DSMZ, medium no. 104 without glucose), supplemented with 1 mM Glc and 1 mM GlcNAc (Carbosynth, Berkshire, UK), 1 mM GlcNAz, 1 mM ManNAz or 1 mM 5-*N*-azidoacetylneuraminic acid (SiaNAz), respectively. The azido sugars were synthesised at Glycom A/S (Hørsholm, Denmark). After incubation under rotation at 37°C for 6 hr, liquid cultures were pelleted and prepared for analysis by flow cytometry or DNA was extracted using the QIAamp Fast DNA stool mini kit (Qiagen) for 16S rRNA sequencing.

4.4 | Analysis of azido sugar incorporation by flow cytometry

After supplementation with azido sugars, bacterial cultures were pelleted, and bacterial cells were washed with PBS. Azide-labelled bacteria were fluorescently tagged by a reaction with an Alexa Fluor™ 488-alkyne dye (Molecular probes®, Thermo Fisher Scientific) using copper-catalysed click chemistry (2 mM $CuSO_4$, 4 mM Tris[(1-benzyl-1*H*-1,2,3-triazol-4-yl)methyl]amine, 5 mM sodium ascorbate, 4.8 μM alkyne dye in PBS [Dumont et al., 2012]) for 1 hr in the dark at room temperature. The specificity of click reactions was monitored through control reactions lacking either azido sugar, alkyne dye or $CuSO_4$. Bacteria were then washed twice in PBS and analysed using a FACSCanto II flow cytometer (BD Bioscience). Separation of azide label-positive and azide label-negative bacteria was done using a FACSAria III cell sorter (BD Bioscience) after GlcNAc or GlcNAz supplementation of caecum slurry cultures of WT and $Il10^{-/-}$ for 6 hr.

4.5 | 16S rRNA next generation sequencing

Bacterial DNA was isolated from caecum content and bacterial cultures using the QIAamp Fast DNA stool mini kit. Sorted bacteria

underwent a proteinase K digest (2% proteinase K in 50 mM KCl, 10 mM Tris Base, pH 8, 0.45% Nonidet P-40, 0.45% Tween 20) for 45 min at 50°C. 16S rRNA was amplified using universal primers 8F and 1492R (Chassard, Goumy, Leclerc, Del'homme, & Bernalier-Donadille, 2007). The 16S rRNA V3-V4 region was amplified in a second PCR using primer V3F 340-356 (5′-CTTTCCCTACACGACG CTCTTCCGATCT-CCTACGGRAGGCAGCAG-3′) and V4R 805-786 (5′-GGA GTT CAG ACG TGT GCT CTT CCG ATC T-GGACTACH VGGGTWTCTAAT-3′) (Schloss, Jenior, Koumpouras, Westcott, & Highlander, 2016). Both primers contained an Illumina adapter at the 5′-end. Sequencing was performed with the Illumina MiSeq platform (Illumina, San Diego) using v2 chemistry and 250x2 read length. Bioinformatic analysis of 16S sequence was performed as previously described (Appert et al., 2020). Briefly, Illumina adaptors and gene-specific primers were removed using atropos (Didion, Martin, & Collins, 2017). Sequences were then processed using the DADA2 pipeline (Callahan et al., 2016), which allows inference of exact amplicon sequence variants (ASVs). Reads pairs were truncated after 231 and 229 nucleotides for forward and reverse reads, respectively. After truncation, reads with expected error rates higher than 4 and 5 for forward and reverse reads were removed. After filtering, error rate learning, ASV inference and denoising, reads were merged with a minimum overlap of 20 bp. Chimeric sequences were identified and removed using "consensus" method and taxonomy assignments were performed using dada2 against SILVA database (v.138) (Glockner et al., 2017). Further analysis was performed using QIIME 1 (Caporaso et al., 2010).

4.6 | Quantitative PCR

Bacteroides spp., *B. acidifaciens* and *B. vulgatus* were quantified as proportion of total bacterial 16S rRNA amplicons by real-time PCR using the KAPA SYBR® FAST qPCR Master Mix Kit (Kapa Biosystems). Cycling conditions were 50 cycles at 95°C for 10 s and 60°C for 30 s after an initial denaturation at 95°C for 3 min. Primer pairs specific for *Bacteroides* spp. (forward: 5′-AAGGTCCCCCACATTGG-3′; reverse: 5′-GAGCCGCAAACTTTCACAA-3′) and total bacteria (515F: 5′-GTGCCAGCMGCCGCGGTAA-3′; 805R: 5′-GACTACCAGGGTA TCTAAT-3′) were described previously (Frank et al., 2007; Franks et al., 1998; Manz, Amann, Ludwig, Vancanneyt, & Schleifer, 1996). Primer pair specific for the recA gene for recombinase A of *B. acidifaciens* (forward: 5″-AACCTGATAACGGTGAGCAGGCG-3′; reverse: 5′- GCTGACAGCCGAGGTCAATTTG-3′) was designed. The lack of significant sequence similarity of the selected primers with unrelated bacterial sequences was confirmed by BLAST analysis. The primers for the *B. vulgatus* sialidase gene Bv-f266 (5″-GGAGGGGAAAGACTTATTTTGC-3′) and Bv-r501 (5′-TTCCACC ACTTCTGCCGAC-3′) were used as described previously (Huang et al., 2015). The $2^{-\Delta Ct}$ method was used to calculate quantification values relative to total bacterial 16S rRNA amplicons (Schmittgen & Livak, 2008).

4.7 | Carbohydrate hydrolase activity assays

The caecum content of 8–10 week-old mice was collected and centrifuged at 16′000 × g for 20 min at 4°C. The resulting supernatants were applied for carbohydrate hydrolase assays. Galactosidase, fucosidase, and *N*-acetylglucosaminidase activities were measured using the colorimetric substrates 4-nitrophenyl α-D-galactopyranoside (Sigma), 4-nitrophenyl β-D-galactopyranoside (Carbosynth), 4-nitrophenyl α-L-fucopyranoside (Carbosynth), 4-nitrophenyl β-L-fucopyranoside (Sigma), 4-nitrophenyl *N*-acetyl-α-D-glucosamine (Carbosynth) and 4-nitrophenyl *N*-acetyl-β-D-glucosamine (Sigma). Sialidase activity was measured using the fluorogenic substrate 2′-(4-methylumbelliferyl)-α-D-*N*-acetylneuraminic acid sodium salt (4MU-NeuNAc; Carbosynth). Assays consisting of 10 μl caecum fluid, 50 μl of 6 mM 4-nitrophenyl-carbohydrate substrate and 190 μl 0.1 M phosphate-buffered saline, pH 6.5 were incubated at 37°C for 30 min. Assays were stopped by addition of 250 μl 0.5 M Na_2CO_3, pH 10.5. Cleaved 4-nitrophenol was measured by colorimetric detection in a microplate reader (Tecan, Infinite M200 Pro) via absorbance measurement at a wavelength of 405 nm. For sialidase activity, assays consisted of 10 μl caecum fluid and 190 μl of 0.1 mM 4MU-NeuNAc in 100 mM Tris-Cl buffer, pH 7.4 incubated at 37°C for 15 min. Assays were stopped by addition of 800 μl of 0.5 M Na_2CO_3, pH 10.5. Cleaved 4-MU was measured by fluorescence detection in a microplate reader (Tecan, Infinite M200 Pro) at an excitation wavelength of 360 nm and an emission wavelength of 440 nm.

4.8 | Quantification of monosaccharides

Caecum samples were isolated and processed as for carbohydrate hydrolase activity assays. The supernatant was filtered through a 0.45 μm cronus HPLC membrane and stored at −20°C before use. 5 μl were injected into a Dionex ICS-5000$^+$ ion chromatography system (Thermo Fisher Scientific) and monosaccharides were separated on a PA1 CarboPac column, 250 × 4 mm, with 10 mM NaOH at a flow rate of 1 ml min^{-1}. Fuc, GalN, GlcN, Gal, Glc, GlcNAc and GalNAc were identified and quantified by comparison with authentic standards. For the quantification of sialic acids, samples were derivatised with 1,2-diamino-4,5-methylene- dioxybenzene (DMB, Sigma-Aldrich) as described previously (Hara et al., 1989). In brief, 3 μl of caecum fluid were incubated with 200 μl of 3.5 mM DMB dihydrochloride in 1.7 M acetic acid containing 375 mM β-mercaptoethanol and 9 mM sodium hydrosulfite at 50°C for 2.5 hr in the dark. The reaction was stopped by adding 800 μl of ice-cold distilled water. Derivatised sialic acids were separated by reversed phase HPLC (Hitachi Chromaster, VWR) on a ODS Hypersil 150 × 3 mm column (Thermo Fisher Scientific) using acetonitrile/methanol/water (9:7:84, v/v/v) as mobile phase at a flow rate of 0.3 ml min^{-1}. Fluorescence of the derivatised products was monitored at 373 nm (excitation) and 448 nm (emission). Neu5Gc, Neu5Ac and Neu5,9Ac$_2$ were identified by comparison to authentic standards.

4.9 | Stimulation of bone marrow-derived dendritic cells

Bone marrow-derived murine dendritic cells were generated following the protocol of Matheu et al. (Matheu, Sen, Cahalan, & Parker, 2008). The water lysis of the red blood cells was replaced by treatment with ammonium-chloride-potassium (ACK) lysing buffer (150 mM NH_4Cl, 10 mM $KHCO_3$, 0.1 mM EDTA). Mature dendritic cells were cultured in Iscove's Modified Dulbecco's Medium (Gibco) containing 10% FCS, 1 mM sodium pyruvate and 1x GlutaMAX™ supplement (Gibco). Cells were stimulated with fixed bacteria, PBS or LPS for 18 hr at 37°C. Before stimulation, *B. acidifaciens* and *B. vulgatus* were grown for 16 hr in PYG supplemented with 5, 10 or 20 mM of either GlcNAc, ManNAc or SiaNAc or PYG medium alone. The density of the supplemented *Bacteroides* species were normalised by OD_{600} measurement and cell counting by cytometry. Equal bacterial counts were fixed in 2% paraformaldehyde for 15 min at room temperature, washed with PBS and co-cultured with dendritic cells in a ratio of 10:1 for 18 hr. Stimulation with O111:B4 *E. coli* LPS was done at a concentration of 100 ng/ml. After stimulation, dendritic cells were stained with fluorochrome-labelled anti-mouse antibodies CD40-APC, CD86-PE and MHC-II-FITC (BioLegend) for 30 min on ice. Cells were analysed using a FACSCanto II flow cytometer (BD Bioscience). Cytokine expression after stimulation was determined by ProcartaPlex™ Multiplex immunoassay (ThermoFisher Scientific) according to the manufacturer's instructions.

4.10 | Isolation and analysis of LPS

LPS was isolated as described by Davis and Goldberg (Davis Jr. & Goldberg, 2012) with minor modifications. In brief, cultures were washed twice with PBS, OD_{600} was measured and cultures diluted to reach equal cell densities. Bacteria were centrifuged at 12′000 x g for 10 min and cell pellets were lysed by boiling in 600 µl of SDS buffer consisting of 2% SDS, 10% glycerol, 2% β-mercaptoethanol in 50 mM Tris–HCl, pH 6.8 for 15 min. After cooling on ice, 2 mg of DNAse I and RNAse A were added and samples were incubated for 30 min at 37°C, then 2 mg proteinase K was added and samples were further incubated overnight at 59°C. Phenol (600 µl) was added, samples were incubated at 65°C for 15 min after vortexing. After cooling on ice, 3 ml of diethylether was added and samples vortexed and spun at 10′000 x g for 10 min. The lower aqueous phase was extracted and the phase separation with phenol and diethylether was repeated once. To each sample, 500 µl of 2X SDS buffer was added prior to performing gel electrophoresis in 14% polyacrylamide gels (Davis Jr. & Goldberg, 2012). LPS was developed by silver staining following the procedure of Fomsgaard et al. (Fomsgaard, Freudenberg, & Galanos, 1990).

CONFLICT OF INTEREST

The authors declare no conflicts of interest.

AUTHOR CONTRIBUTIONS

Gisela Adrienne Weiss and Thierry Hennet designed the study. Nikolay Khanzhin synthesised the azido sugars, Gisela Adrienne Weiss and Tobias Hasler analysed caecum monosaccharides and carbohydrate hydrolase activities, Thomas Grabinger isolated LPS and performed dendritic cells assays with Gisela Adrienne Weiss and Tobias Hasler. Gisela Adrienne Weiss and Jesús Glaus Garzon performed FACS-based bacterial sorting. Gisela Adrienne Weiss, Anna Greppi and Christophe Lacroix analysed 16S rRNA sequencing data. Gisela Adrienne Weiss, Thomas Grabinger, Tobias Hasler and Anna Greppi prepared the figures. Gisela Adrienne Weiss, Thomas Grabinger and Thierry Hennet wrote the manuscript. All authors contributed to the revision of the manuscript. Thierry Hennet secured the funding.

DATA AVAILABILITY STATEMENT

The data that support the findings of this study are available from the corresponding author upon request.

ORCID

Gisela Adrienne Weiss https://orcid.org/0000-0002-5983-5569
Thomas Grabinger https://orcid.org/0000-0003-3198-0868
Jesus Glaus Garzon https://orcid.org/0000-0002-6820-2050
Tobias Hasler https://orcid.org/0000-0001-9133-584X
Christophe Lacroix https://orcid.org/0000-0003-4360-2020
Thierry Hennet https://orcid.org/0000-0002-7276-737X

REFERENCES

Agard, N. J., Baskin, J. M., Prescher, J. A., Lo, A., & Bertozzi, C. R. (2006). A comparative study of bioorthogonal reactions with azides. *ACS Chemical Biology*, 1(10), 644–648.

Ahn, D. H., Crawley, S. C., Hokari, R., Kato, S., Yang, S. C., Li, J. D., & Kim, Y. S. (2005). TNF-alpha activates MUC2 transcription via NF-kappaB but inhibits via JNK activation. *Cellular Physiology and Biochemistry*, 15(1–4), 29–40. https://doi.org/10.1159/000083636

Appert, O., Garcia, A. R., Frei, R., Roduit, C., Constancias, F., Neuzil-Bunesova, V., … Schwab, C. (2020). Initial butyrate producers during infant gut microbiota development are endospore formers. *Environmental Microbiology*, 22, 3909–3921. https://doi.org/10.1111/1462-2920.15167

Assis, R. A. B., Polloni, L. C., Patane, J. S. L., Thakur, S., Felestrino, E. B., Diaz-Caballero, J., … Moreira, L. M. (2017). Identification and analysis of seven effector protein families with different adaptive and evolutionary histories in plant-associated members of the Xanthomonadaceae. *Scientific Reports*, 7(1), 16133. https://doi.org/10.1038/s41598-017-16325-1

Baker, P., Whitfield, G. B., Hill, P. J., Little, D. J., Pestrak, M. J., Robinson, H., … Howell, P. L. (2015). Characterization of the *Pseudomonas aeruginosa* glycoside hydrolase PslG reveals that its levels are critical for Psl polysaccharide biosynthesis and biofilm formation. *The Journal of Biological Chemistry*, 290(47), 28374–28387. https://doi.org/10.1074/jbc.M115.674929

Bergstrom, K. S., & Xia, L. (2013). Mucin-type O-glycans and their roles in intestinal homeostasis. *Glycobiology*, *23*(9), 1026–1037. https://doi.org/10.1093/glycob/cwt045

Brigham, C., Caughlan, R., Gallegos, R., Dallas, M. B., Godoy, V. G., & Malamy, M. H. (2009). Sialic acid (N-acetyl neuraminic acid) utilization by *Bacteroides fragilis* requires a novel N-acetyl mannosamine epimerase. *Journal of Bacteriology*, *191*(11), 3629–3638. https://doi.org/10.1128/JB.00811-08

Callahan, B. J., McMurdie, P. J., Rosen, M. J., Han, A. W., Johnson, A. J., & Holmes, S. P. (2016). DADA2: High-resolution sample inference from Illumina amplicon data. *Nature Methods*, *13*(7), 581–583. https://doi.org/10.1038/nmeth.3869

Caporaso, J. G., Kuczynski, J., Stombaugh, J., Bittinger, K., Bushman, F. D., Costello, E. K., ... Knight, R. (2010). QIIME allows analysis of high-throughput community sequencing data. *Nature Methods*, *7*(5), 335–336. https://doi.org/10.1038/nmeth.f.303 nmeth.f.303 [pii].

Chassard, C., Goumy, V., Leclerc, M., Del'homme, C., & Bernalier-Donadille, A. (2007). Characterization of the xylan-degrading microbial community from human faeces. *FEMS Microbiology Ecology*, *61*(1), 121–131. https://doi.org/10.1111/j.1574-6941.2007.00314.x

Davies, H. S., Singh, P., Deckert-Gaudig, T., Deckert, V., Rousseau, K., Ridley, C. E., ... Blanch, E. W. (2016). Secondary structure and glycosylation of mucus glycoproteins by Raman spectroscopies. *Analytical Chemistry*, *88*(23), 11609–11615. https://doi.org/10.1021/acs.analchem.6b03095

Davis, M. R., Jr., & Goldberg, J. B. (2012). Purification and visualization of lipopolysaccharide from gram-negative bacteria by hot aqueous-phenol extraction. *Journal of Visualized Experiments*, (63), 3916. https://doi.org/10.3791/3916

Didion, J. P., Martin, M., & Collins, F. S. (2017). Atropos: Specific, sensitive, and speedy trimming of sequencing reads. *PeerJ*, *5*, e3720. https://doi.org/10.7717/peerj.3720

Dumont, A., Malleron, A., Awwad, M., Dukan, S., & Vauzeilles, B. (2012). Click-mediated labeling of bacterial membranes through metabolic modification of the lipopolysaccharide inner core. *Angewandte Chemie (International Ed. in English)*, *51*(13), 3143–3146. https://doi.org/10.1002/anie.201108127

Duncan, S. H., Hold, G. L., Harmsen, H. J., Stewart, C. S., & Flint, H. J. (2002). Growth requirements and fermentation products of Fusobacterium prausnitzii, and a proposal to reclassify it as Faecalibacterium prausnitzii gen. nov., comb. nov. *International Journal of Systematic and Evolutionary Microbiology*, *52*(Pt 6), 2141–2146. https://doi.org/10.1099/00207713-52-6-2141

El Kaoutari, A., Armougom, F., Gordon, J. I., Raoult, D., & Henrissat, B. (2013). The abundance and variety of carbohydrate-active enzymes in the human gut microbiota. *Nature Reviews. Microbiology*, *11*(7), 497–504. https://doi.org/10.1038/nrmicro3050

Etzold, S., & Juge, N. (2014). Structural insights into bacterial recognition of intestinal mucins. *Current Opinion in Structural Biology*, *28C*, 23–31. https://doi.org/10.1016/j.sbi.2014.07.002

Fletcher, C. M., Coyne, M. J., Villa, O. F., Chatzidaki-Livanis, M., & Comstock, L. E. (2009). A general O-glycosylation system important to the physiology of a major human intestinal symbiont. *Cell*, *137*(2), 321–331. https://doi.org/10.1016/j.cell.2009.02.041

Fomsgaard, A., Freudenberg, M. A., & Galanos, C. (1990). Modification of the silver staining technique to detect lipopolysaccharide in polyacrylamide gels. *Journal of Clinical Microbiology*, *28*(12), 2627–2631.

Frank, D. N., St Amand, A. L., Feldman, R. A., Boedeker, E. C., Harpaz, N., & Pace, N. R. (2007). Molecular-phylogenetic characterization of microbial community imbalances in human inflammatory bowel diseases. *Proceedings of the National Academy of Sciences of the United States of America*, *104*(34), 13780–13785. https://doi.org/10.1073/pnas.0706625104

Franks, A. H., Harmsen, H. J., Raangs, G. C., Jansen, G. J., Schut, F., & Welling, G. W. (1998). Variations of bacterial populations in human feces measured by fluorescent in situ hybridization with group-specific 16S rRNA-targeted oligonucleotide probes. *Applied and Environmental Microbiology*, *64*(9), 3336–3345.

Geva-Zatorsky, N., Alvarez, D., Hudak, J. E., Reading, N. C., Erturk-Hasdemir, D., Dasgupta, S., ... Kasper, D. L. (2015). In vivo imaging and tracking of host-microbiota interactions via metabolic labeling of gut anaerobic bacteria. *Nature Medicine*, *21*(9), 1091–1100. https://doi.org/10.1038/nm.3929

Glockner, F. O., Yilmaz, P., Quast, C., Gerken, J., Beccati, A., Ciuprina, A., ... Ludwig, W. (2017). 25 years of serving the community with ribosomal RNA gene reference databases and tools. *Journal of Biotechnology*, *261*, 169–176. https://doi.org/10.1016/j.jbiotec.2017.06.1198

Goto, Y., Obata, T., Kunisawa, J., Sato, S., Ivanov, I. I., Lamichhane, A., ... Kiyono, H. (2014). Innate lymphoid cells regulate intestinal epithelial cell glycosylation. *Science*, *345*(6202), 1254009. https://doi.org/10.1126/science.1254009

Grabinger, T., Glaus Garzon, J. F., Hausmann, M., Geirnaert, A., Lacroix, C., & Hennet, T. (2019). Alleviation of intestinal inflammation by oral supplementation with 2-fucosyllactose in mice. *Frontiers in Microbiology*, *10*, 1385. https://doi.org/10.3389/fmicb.2019.01385

Hansson, G. C. (2012). Role of mucus layers in gut infection and inflammation. *Current Opinion in Microbiology*, *15*(1), 57–62. https://doi.org/10.1016/j.mib.2011.11.002

Hara, S., Yamaguchi, M., Takemori, Y., Furuhata, K., Ogura, H., & Nakamura, M. (1989). Determination of mono-O-acetylated N-acetylneuraminic acids in human and rat sera by fluorometric high-performance liquid chromatography. *Analytical Biochemistry*, *179*(1), 162–166.

Harvey, H. A., Swords, W. E., & Apicella, M. A. (2001). The mimicry of human glycolipids and glycosphingolipids by the lipooligosaccharides of pathogenic neisseria and haemophilus. *Journal of Autoimmunity*, *16*(3), 257–262. https://doi.org/10.1006/jaut.2000.0477

Hashimoto, M., Kirikae, F., Dohi, T., Adachi, S., Kusumoto, S., Suda, Y., ... Kirikae, T. (2002). Structural study on lipid A and the O-specific polysaccharide of the lipopolysaccharide from a clinical isolate of Bacteroides vulgatus from a patient with Crohn's disease. *European Journal of Biochemistry*, *269*(15), 3715–3721. https://doi.org/10.1046/j.1432-1033.2002.03062.x

Hokari, R., Lee, H., Crawley, S. C., Yang, S. C., Gum, J. R., Jr., Miura, S., & Kim, Y. S. (2005). Vasoactive intestinal peptide upregulates MUC2 intestinal mucin via CREB/ATF1. *American Journal of Physiology. Gastrointestinal and Liver Physiology*, *289*(5), G949–G959. https://doi.org/10.1152/ajpgi.00142.2005

Huang, Y. L., Chassard, C., Hausmann, M., von Itzstein, M., & Hennet, T. (2015). Sialic acid catabolism drives intestinal inflammation and microbial dysbiosis in mice. *Nature Communications*, *6*, 8141. https://doi.org/10.1038/ncomms9141

Hungate, R. E. (1969). Chapter IV a roll tube method for cultivation of strict anaerobes. *Methods in Microbiology*, *3*, 117–132.

Jacobson, A. N., Choudhury, B. P., & Fischbach, M. A. (2018). The biosynthesis of lipooligosaccharide from bacteroides thetaiotaomicron. *MBio*, *9*(2), e02289–17. https://doi.org/10.1128/mBio.02289-17

Johansson, M. E., Phillipson, M., Petersson, J., Velcich, A., Holm, L., & Hansson, G. C. (2008). The inner of the two Muc2 mucin-dependent mucus layers in colon is devoid of bacteria. *Proceedings of the National Academy of Sciences of the United States of America*, *105*(39), 15064–15069. https://doi.org/10.1073/pnas.0803124105

Konopka, J. B. (2012). N-acetylglucosamine (GlcNAc) functions in cell signaling. *Scientifica (Cairo)*, *2012*, 1–15. https://doi.org/10.6064/2012/489208

Koropatkin, N. M., Cameron, E. A., & Martens, E. C. (2012). How glycan metabolism shapes the human gut microbiota. *Nature Reviews. Microbiology*, *10*(5), 323–335. https://doi.org/10.1038/nrmicro2746

Kuhn, R., Lohler, J., Rennick, D., Rajewsky, K., & Muller, W. (1993). Interleukin-10-deficient mice develop chronic enterocolitis. *Cell*, *75*(2), 263–274.

Kyogashima, M., Ginsburg, V., & Krivan, H. C. (1989). *Escherichia coli* K99 binds to N-glycolylsialoparagloboside and N-glycolyl-GM3 found in piglet small intestine. *Archives of Biochemistry and Biophysics*, 270(1), 391–397.

Lee, H. S., Han, S. Y., Ryu, K. Y., & Kim, D. H. (2009). The degradation of glycosaminoglycans by intestinal microflora deteriorates colitis in mice. *Inflammation*, 32(1), 27–36. https://doi.org/10.1007/s10753-008-9099-6

Lupp, C., Robertson, M. L., Wickham, M. E., Sekirov, I., Champion, O. L., Gaynor, E. C., & Finlay, B. B. (2007). Host-mediated inflammation disrupts the intestinal microbiota and promotes the overgrowth of Enterobacteriaceae. *Cell Host & Microbe*, 2(2), 119–129. S1931-3128(07)00157-6 [pii]. https://doi.org/10.1016/j.chom.2007.06.010

Maharshak, N., Packey, C. D., Ellermann, M., Manick, S., Siddle, J. P., Huh, E. Y., ... Carroll, I. M. (2013). Altered enteric microbiota ecology in interleukin 10-deficient mice during development and progression of intestinal inflammation. *Gut Microbes*, 4(4), 316–324. https://doi.org/10.4161/gmic.25486

Mahdavi, J., Pirinccioglu, N., Oldfield, N. J., Carlsohn, E., Stoof, J., Aslam, A., ... Ala'Aldeen, D. A. (2014). A novel O-linked glycan modulates Campylobacter jejuni major outer membrane protein-mediated adhesion to human histo-blood group antigens and chicken colonization. *Open Biology*, 4, 130202. https://doi.org/10.1098/rsob.130202

Manz, W., Amann, R., Ludwig, W., Vancanneyt, M., & Schleifer, K. H. (1996). Application of a suite of 16S rRNA-specific oligonucleotide probes designed to investigate bacteria of the phylum cytophaga-flavobacter-bacteroides in the natural environment. *Microbiology*, 142 (Pt 5), 1097–1106. https://doi.org/10.1099/13500872-142-5-1097

Martens, E. C., Chiang, H. C., & Gordon, J. I. (2008). Mucosal glycan foraging enhances fitness and transmission of a saccharolytic human gut bacterial symbiont. *Cell Host & Microbe*, 4(5), 447–457. https://doi.org/10.1016/j.chom.2008.09.007

Martens, E. C., Lowe, E. C., Chiang, H., Pudlo, N. A., Wu, M., McNulty, N. P., ... Gordon, J. I. (2011). Recognition and degradation of plant cell wall polysaccharides by two human gut symbionts. *PLoS Biology*, 9(12), e1001221. https://doi.org/10.1371/journal.pbio.1001221

Matheu, M. P., Sen, D., Cahalan, M. D., & Parker, I. (2008). Generation of bone marrow derived murine dendritic cells for use in 2-photon imaging. *Journal of Visualized Experiments*, (17), 773. https://doi.org/10.3791/773

Mazmanian, S. K., Round, J. L., & Kasper, D. L. (2008). A microbial symbiosis factor prevents intestinal inflammatory disease. *Nature*, 453(7195), 620–625. nature07008 [pii]. https://doi.org/10.1038/nature07008

Neff, C. P., Rhodes, M. E., Arnolds, K. L., Collins, C. B., Donnelly, J., Nusbacher, N., ... Lozupone, C. A. (2016). Diverse intestinal bacteria contain putative Zwitterionic capsular polysaccharides with anti-inflammatory properties. *Cell Host & Microbe*, 20(4), 535–547. https://doi.org/10.1016/j.chom.2016.09.002

Ng, K. M., Ferreyra, J. A., Higginbottom, S. K., Lynch, J. B., Kashyap, P. C., Gopinath, S., ... Sonnenburg, J. L. (2013). Microbiota-liberated host sugars facilitate post-antibiotic expansion of enteric pathogens. *Nature*, 502(7469), 96–99. https://doi.org/10.1038/nature12503

Pickard, J. M., Maurice, C. F., Kinnebrew, M. A., Abt, M. C., Schenten, D., Golovkina, T. V., ... Chervonsky, A. V. (2014). Rapid fucosylation of intestinal epithelium sustains host-commensal symbiosis in sickness. *Nature*, 514(7524), 638–641. https://doi.org/10.1038/nature13823

Raetz, C. R., & Whitfield, C. (2002). Lipopolysaccharide endotoxins. *Annual Review of Biochemistry*, 71, 635–700. https://doi.org/10.1146/annurev.biochem.71.110601.135414

Ravcheev, D. A., & Thiele, I. (2017). Comparative genomic analysis of the human gut microbiome reveals a broad distribution of metabolic pathways for the degradation of host-synthetized Mucin Glycans and utilization of Mucin-Derived monosaccharides. *Frontiers in Genetics*, 8, 111. https://doi.org/10.3389/fgene.2017.00111

Sambrook, J., & Russel, D. (2001). *Molecular cloning: A laboratory manual*. Woodbury, NY: Spring Harbor Laboratory Press.

Schloss, P. D., Jenior, M. L., Koumpouras, C. C., Westcott, S. L., & Highlander, S. K. (2016). Sequencing 16S rRNA gene fragments using the PacBio SMRT DNA sequencing system. *PeerJ*, 4, e1869. https://doi.org/10.7717/peerj.1869

Schmittgen, T. D., & Livak, K. J. (2008). Analyzing real-time PCR data by the comparative C(T) method. *Nature Protocols*, 3(6), 1101–1108.

Tailford, L. E., Crost, E. H., Kavanaugh, D., & Juge, N. (2015). Mucin glycan foraging in the human gut microbiome. *Frontiers in Genetics*, 6, 81. https://doi.org/10.3389/fgene.2015.00081

Thomer, L., Becker, S., Emolo, C., Quach, A., Kim, H. K., Rauch, S., ... Missiakas, D. (2014). N-acetylglucosaminylation of serine-aspartate repeat proteins promotes *Staphylococcus aureus* bloodstream infection. *The Journal of Biological Chemistry*, 289(6), 3478–3486. https://doi.org/10.1074/jbc.M113.532655

Thomsson, K. A., Holmen-Larsson, J. M., Angstrom, J., Johansson, M. E., Xia, L., & Hansson, G. C. (2012). Detailed O-glycomics of the Muc2 mucin from colon of wild-type, core 1- and core 3-transferase-deficient mice highlights differences compared with human MUC2. *Glycobiology*, 22(8), 1128–1139. https://doi.org/10.1093/glycob/cws083 cws083 [pii].

Uehara, T., & Park, J. T. (2004). The N-acetyl-D-glucosamine kinase of *Escherichia coli* and its role in murein recycling. *Journal of Bacteriology*, 186(21), 7273–7279. https://doi.org/10.1128/JB.186.21.7273-7279.2004

Weiss, G. A., & Hennet, T. (2017). Mechanisms and consequences of intestinal dysbiosis. *Cellular and Molecular Life Sciences*, 74(16), 2959–2977. https://doi.org/10.1007/s00018-017-2509-x

Yang, W. H., Heithoff, D. M., Aziz, P. V., Sperandio, M., Nizet, V., Mahan, M. J., & Marth, J. D. (2017). Recurrent infection progressively disables host protection against intestinal inflammation. *Science*, 358 (6370), eaao5610. https://doi.org/10.1126/science.aao5610

SUPPORTING INFORMATION

Additional supporting information may be found online in the Supporting Information section at the end of this article.